

RESEARCH PAPER

Modelling Radial Oscillations of a Bubble in a Spherical Liquid-Filled Elastic Solid.

Dana A. Mohammedameen¹, Kawa M.A. MANMI¹, Waleed H. Aziz¹

¹ Department of Mathematics, College of Science, Salahaddin University-Erbil, Kurdistan Region, Iraq

ABSTRACT:

In this paper, the equation of spherical bubble oscillations in Newtonian and viscous fluid with considering compressible fluid flow in a spherical liquid-filled elastic solid was developed. The exact solution of the linearisation and the numerical solution of the equation has been derived and compared. Then numerical calculations are performed to investigate the effects of compressibility parameter ε_* for gas and acoustic bubbles. the amplitude of bubble radius oscillations increases with ε_* and the effects of ε_* is accumulating with time. Further, the discrepancy between the exact and numerical solutions increases with time when $\varepsilon_* = 0.08$. However, the difference was not changed when the ε_* is smaller than 0.08. Dual frequency is also considered in the acoustic environment.

KEY WORDS: Spherical bubble, Bubble oscillations, Acoustic wave, Elastic solid, Rayleigh-Plesset equation.

DOI: <http://dx.doi.org/10.21271/ZJPAS.34.6.3>

ZJPAS (2022) , 34(6);20-27 .

1. INTRODUCTION:

Cavitation in fluid dynamics is a complicated phenomenon that often occurs in many natural and manmade processes induced by rapid changes in flux situations. For example when a fluid passes through a cross section reduction (like in a valve) or after a sudden increase in flow velocity imposed by, for instance, a ship propeller (Franc and Michel, 2006). Cavitation traditionally was regarded as an unwanted phenomenon particularly in the machinery engines as it produces many negative effects including vibration, noise and efficiency reduction (Bosschers, 2018, Korkut and Atlar, 2012, Franc and Michel, 2006).

However, in the last three decades several applications of cavitation have been proposed. These include the production of ground purification methods, biomedical treatments such as the disintegration of kidney stones or elimination of microorganisms (Duryea et al., 2015, Duryea et al., 2010), and chemical processes such as sonochemistry and sonoluminescence (Nigmatulin et al., 1999, Crum et al., 1998, Yusof et al., 2022, Zhou et al., 2013). Although, in most situations' cavitation represents a cloud of tiny bubbles, understanding a single bubble dynamic is essential and crucial. On the other hand, bubble tend to spherical shape entirely or partially due to surface tension force. Therefore, understanding single spherical bubble dynamics is fundamental area for cavitation phenomena.

The first mathematical model of the spherical bubble was formulated by Rayleigh in 1917 (Rayleigh, 1917). The model is based on the continuity equation with neglects viscosity and surface tension effects. However, these

* Corresponding Author:

Dana Ahmed Mohammedameen

E-mail: dana.muhammedameen@su.edu.krd

Article History:

Received: 13/06/2022

Accepted: 02/08/2022

Published: 20/12 /2022

assumptions might be only validated in a certain situation for instance in bubbles with a radius of $O(m)$. Plesset developed Rayleigh’s work in 1949 to include some other effects, such as viscosity and surface tension effects in an incompressible fluid (Plesset and Prosperetti, 1977). In 1956, Keller and Kolodner (Keller and Kolodner, 1956) extended Rayleigh-Plesset formula for the Keller-Miksis equation of the oscillations of a spherical bubble in a compressible liquid (Lauterborn and Kurz, 2010).

Most recently, gas and acoustic bubble oscillations (dynamics) inside a liquid-filled elastic solid have been great attention by researchers due to applications in plants (Wang, 2017, Cochard, 2006, Tyree and Sperry, 1989, Stroock et al., 2014, Larter et al., 2015, Jensen et al., 2016). By considering the interaction between the bubble gas expansion/collapse, the liquid flow produced, and the elastic confinement deformation (Liu et al., 2018). They studied shape modes of non-spherical oscillations. The equations of strain and stress fields in the solid medium around it were considered by (Doynikov et al., 2018a). The major process of attenuation, according to (Drysdale et al., 2017), is related to wave propagation in solids.

The remainder of the article is organized as follows: In section 2 physical and mathematical model for spherical bubble oscillations inside spherical elastic solid is derived. The nonlinear governing equation of section 2 for small amplitude of oscillations is linearized and natural frequency for the linearized equation is illustrated in section 3. In section 4, the nondimensional variables are defined to dimensionless the governing equations. Section 5 is focused on the numerical results of the gas/ acoustic bubble oscillations a spherical liquid-filled elastic solid. The conclusions are summarized in section 6.

2. PHYSICAL AND MATHEMATICAL MODEL

In this paper, we assume that a pre-existing spherical bubble with a radius R_0 in a Newtonian liquid is confined within a spherical elastic solid with a radius R_{c0} . The bubble starts to oscillate spherically when the gas pressure inside the bubble is not equal to the liquid pressure. To formulate a simplified mathematical model which is based on the mass and momentum

conservations with neglecting mass and heat transfer along the interfaces, the instantaneous radius for bubble and elastic solid are denoted by $R(t)$ and $R_c(t)$, respectively, as it can be seen in Figure 1, where t is time.

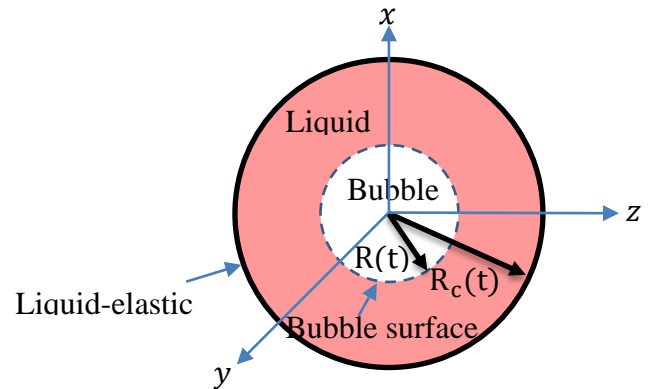


Fig. 1. Schematic of the spherical bubble in a liquid confined with spherical elastic solid. The radius of the bubble is $R(t)$ and the elastic cavity is $R_c(t)$.

The mass conservation with the combination of the material derivative (Acheson, 1991, Batchelor and Batchelor, 2000, Yasui, 2018) of the liquid flow is written as

$$\begin{aligned} \frac{\partial \rho}{\partial t} + \nabla \cdot (\rho \mathbf{u}) &= \frac{\partial \rho}{\partial t} + (\mathbf{u} \cdot \nabla) \rho + \rho \nabla \cdot \mathbf{u} \\ &= \frac{d\rho}{dt} + \rho \nabla \cdot \mathbf{u} = 0, \end{aligned} \quad (1)$$

where ρ and \mathbf{u} are density and velocity field of the liquid and $\nabla = (\partial / \partial x, \partial / \partial y, \partial / \partial z)$ in Cartesian co-ordinates (x, y, z) .

In the spherical coordinate (r, θ, ϕ) with $\mathbf{u} = (u, u_\theta, u_\phi)$, equation (1) becomes

$$\begin{aligned} \frac{d\rho}{dt} + \rho \nabla \cdot \mathbf{u} &= \frac{d\rho}{dt} + \frac{\rho}{r^2} \frac{\partial(r^2 u)}{\partial r} \\ &+ \frac{\rho}{r \sin(\theta)} \frac{\partial}{\partial \theta} (u_\theta \sin(\theta)) + \frac{\rho}{r \sin(\theta)} \frac{\partial u_\phi}{\partial \phi} = 0. \end{aligned} \quad (2)$$

It is assumed that the bubble and the elastic cavity are perfectly spherically symmetric. Therefore, the partial derivative of any variable according to the θ and ϕ coordinates is equal to zero. We get

$$\frac{\rho}{r^2} \frac{\partial(r^2 u)}{\partial r} = -\frac{d\rho}{dt} = -\frac{d\rho}{dp_l} \frac{dp_l}{dt}, \quad (3)$$

Where p_l is pressure of the liquid, $\frac{d\rho}{dt} = \frac{d\rho}{dp_l} \frac{dp_l}{dt}$ and $\frac{d\rho}{dp} = c^2$ is the speed of sound in the liquid. We get

$$\frac{1}{r^2} \frac{\partial(r^2 u)}{\partial r} = -\frac{1}{c^2 \rho} \frac{dp_l}{dt}. \quad (4)$$

The speed of sound and the density of the typical liquid (water) can be approximated by 1500 m/s

and 1000 kg/m^3 , respectively. Therefore, $1/(c^2\rho) \approx 6.6667 * 10^{-7}$. Hence, the right side of the equation of (4) is very small and could be negligible. However, this small term could be significant in a certain regime. Based on this, we assume that $-\frac{1}{c^2\rho} \frac{dp}{dt} \approx \varepsilon(t, r) \approx \varepsilon$, where $\varepsilon \ll 1$.

Now equation (4) reduces to

$$\frac{1}{r^2} \frac{d(r^2u)}{dr} = \varepsilon. \tag{5}$$

The ordinary differential equation (5) is separable; it can be solved simply by taking integral for both sides,

$$r^2u = \frac{\varepsilon r^3}{3} + c. \tag{6}$$

To find the arbitrary constant c , we use the instantaneous bubble radius at time t which means $r = R(t)$ and $dr/dt = \dot{R} = u$ at the bubble surface

$$c = R^2\dot{R} - \frac{\varepsilon R^3}{3}. \tag{7}$$

By substituting c in (6), we have

$$u = \frac{\varepsilon r}{3} + \frac{R^2\dot{R}}{r^2} - \frac{\varepsilon R^3}{3r^2}. \tag{8}$$

The momentum conservation (Navier-Stokes equation) for a compressible Newtonian and irrotational fluid (Marion and Temam, 1998) is written as

$$\rho \left(\frac{\partial \mathbf{u}}{\partial t} + \mathbf{u} \cdot \nabla \mathbf{u} \right) = -\nabla p_l + \mu \nabla^2 \mathbf{u} + \frac{\mu}{3} \nabla (\nabla \cdot \mathbf{u}), \tag{9}$$

where μ and p_l are the viscosity pressure of the liquid. Based on the assumptions of the sphericity and symmetricity, θ and ϕ components of equation (9) in the spherical coordinate system vanish. Therefore, r -component reads

$$\rho \left(\frac{\partial u}{\partial t} + u \frac{\partial u}{\partial r} \right) = -\frac{\partial p_l}{\partial r} + \mu \left(\frac{1}{r} \frac{\partial^2 (ru)}{\partial r^2} - \frac{2u}{r^2} \right) + \frac{\mu}{3} \frac{\partial}{\partial r} \left(\frac{1}{r^2} \frac{\partial (r^2u)}{\partial r} \right), \tag{10}$$

Substituting (8) in (10) we get

$$\rho \left(\frac{9R^2\dot{R} + 18R\dot{R}^2 - 12\varepsilon R^2\dot{R} + \varepsilon^2 R^3}{9r^2} + \frac{\varepsilon^2 r}{9} + \frac{12\varepsilon R^5\dot{R} - 18R^4\dot{R}^2 - 2\varepsilon^2 R^6}{9r^5} \right) = -\frac{\partial p_l}{\partial r}. \tag{11}$$

Integrating equation (11) with respect to r from R to R_c leads to

$$p_{1b} - p_{1c} = \frac{\rho}{9} \left(\frac{\varepsilon^2}{2} (R_c^2 - R^2) - (R^3 \varepsilon^2 \right.$$

$$\left. - 12\varepsilon R^2\dot{R} + 9R^2\dot{R} + 18R\dot{R}^2 \right) \left(\frac{1}{R_c} - \frac{1}{R} \right) + (R^6 \varepsilon^2 - 6R^5\dot{R} + 9R^4\dot{R}^2) \left(\frac{1}{2R_c^4} - \frac{1}{2R^4} \right). \tag{12}$$

where p_{1b} is the liquid pressure of the bubble at the interface and p_{1c} is the liquid pressure at the elastic solid surface. Suppose that gas bubble undergoes an adiabatic or isothermal process, the pressure inside bubble p_B is given by

$$p_B = p_v + P_{g_0} \left(\frac{R_0}{R} \right)^{3\gamma}, \tag{13}$$

where p_v is the partial vapour pressure and P_{g_0} is the initial partial pressure of the gas bubble and γ is the specific heat ratio. The equation of the pressure at the bubble interface from liquid and gas sides can be expressed as p_{1b} related to the interior pressure of the bubble is P_B . It is expressed as

$$p_{1b} = -P_A + p_B - \frac{2\sigma}{R} - 4\mu \frac{\dot{R}}{R}, \tag{14}$$

where σ is the surface tension of the liquid and P_A is the acoustic wave pressure (details in section 5.3).

To find the relation between the bubble volume and the cavity volume we followed the works in (Wang, 2017, Doinikov et al., 2018b, Doinikov et al., 2018a, Liu et al., 2018). They assumed that the volume change of the cavity is linear to the pressure fluctuation at the confinement wall, and the instantaneous volume of the cavity is V_c and its initial value denoted by V_{c0} respectively. The pressure of transient between solid and the liquid is p_{lc} and the pressure of the solid is P_∞ , when the bulk modulus of the elastic confinement is K_c , then

$$V_c - V_{c0} = \frac{V_{c0}}{K_c} (p_{lc} - P_\infty). \tag{15}$$

The change in volume of liquid is also considered to be proportionate to the variation in pressure at the constriction wall. Suppose that V_l is the continuous volume of the liquid and V_{l0} is the initial volume and the bulk modulus of the liquid is K_l , which gives

$$V_l - V_{l0} = \frac{V_{l0}}{K_l} (p_{lc} - P_\infty). \tag{16}$$

It is noted that the cavity volume is equal to the sum of the liquid and bubble volumes, where the volume of the transient bubble is V_b and initially is V_{b0} , respectively then

$$V_{c0} = V_{l0} + V_{b0}, \quad V_c = V_l + V_b, \tag{17}$$

By combining (15), (16) and (17), we get

$$V_b - V_{b0} = V_c - V_{c0} - (V_l - V_{l0}) = \frac{V_{c0}}{K_c} (p_{lc} - P_\infty) - \frac{V_{l0}}{K_l} (p_{lc} - P_\infty). \tag{18}$$

If $V_{b0} \ll V_{c0}$ or $V_{b0} \approx 0$, then $V_{c0} = V_{l0}$, we obtain

$$p_{lc} = K \frac{V_b - V_{b0}}{V_{c0}} + P_\infty = K \frac{R^3 - R_0^3}{R_{c0}^3} + P_\infty, \quad (19)$$

where $K = \left(\frac{1}{K_c} - \frac{1}{K_l}\right)$ and R_{c0} is the initial radius of the cavity. We write K as termed as the effect bulk modulus for the system, which increases with the bulk modulus of the liquid K_l and the bulk modulus of the confinement K_c where the bulk modulus is defined as the relative of the changing pressure by changing the volume (Aritan, 2006).

We substitute p_{lc} into (15). Then we get the relation between bubble radius and cavity radius

$$V_c - V_{c0} = \frac{K}{K_c} (V_b - V_{b0}),$$

or

$$R_c^3 - R_{c0}^3 = \frac{K}{K_c} (R_b^3 - R_{b0}^3). \quad (20)$$

By combining (14), (19) and (12), we get the Rayleigh-Plesset equation for a confined bubble

$$K \frac{R^3 - R_0^3}{R_{c0}^3} + P_\infty + P_A - p_v - P_{g0} \left(\frac{R_0}{R}\right)^{3\gamma} + \frac{2\sigma}{R} + 4\mu \frac{\dot{R}}{R} = -\frac{\rho}{9} \left(\frac{\varepsilon^2}{2} (R_c^2 - R^2) - (R^3 \varepsilon^2 - 12R^2 \dot{R} \varepsilon + 9R^2 \ddot{R} + 18R \dot{R}^2) \left(\frac{1}{R_c} - \frac{1}{R}\right) + (R^6 \varepsilon^2 - 6R^5 \dot{R} \varepsilon + 9R^4 \dot{R}^2) \left(\frac{1}{2R_c^4} - \frac{1}{2R^4}\right) \right). \quad (21)$$

If we set $\varepsilon = 0$, then equation (21) reduces to (Liu, Wang, & Zhang, 2018; Wang, 2017)

$$K \frac{R^3 - R_0^3}{R_{c0}^3} + P_\infty + P_A - p_v - P_{g0} \left(\frac{R_0}{R}\right)^{3\gamma} + \frac{2\sigma}{R} + 4\mu \frac{\dot{R}}{R} = \frac{\rho}{9} \left((9R^2 \ddot{R} + 18R \dot{R}^2) \left(\frac{1}{R_c} - \frac{1}{R}\right) - 9R^4 \dot{R}^2 \left(\frac{1}{2R_c^4} - \frac{1}{2R^4}\right) \right). \quad (22)$$

Further, if R_{c0} approaches to ∞ in (22), then equation (22) will be reduced to the Rayleigh-Plesset equation (Rayleigh, 1917) for a bubble in an unbounded liquid.

$$P_\infty - p_v - P_{g0} \left(\frac{R_0}{R}\right)^{3\gamma} + P_A + \frac{2\sigma}{R} + 4\mu \frac{\dot{R}}{R} = -\rho \left(R^2 \ddot{R} + \frac{3R\dot{R}^2}{2} \right). \quad (23)$$

3. MODEL LINEARIZATION

In this section, equation (21) is linearised by linear perturbation theory. Then an exact solution of the linear solution is derived. To do this, by setting

$R = R_0(1 + x)$, where $x = \mathcal{O}(P_A)$ and $P_A \ll 1$ is the dimensionless amplitude of the pressure perturbation in the Rayleigh-Plesset equation of a bubble in a confinement (21) and using binomial series, we obtain

$$\begin{aligned} & \frac{KR_0^3}{R_{c0}^3} (3x + 3x^2 + x^3) + P_\infty + P_A - p_v - P_{g0} \left(1 - 3\gamma x + \frac{3}{2}\gamma(3\gamma + 1)x^2 + \dots\right) + \frac{2\sigma}{R_0} (1 - x + x^2 + \dots) + 4\mu \dot{x} (1 - x + x^2 + \dots) \\ & = -\frac{\rho}{9} \left(\frac{\varepsilon^2 R_0^2 (1 + 2x + x^2)}{2} \left(\frac{R_{c0}^2}{R_0^2} - 1\right) - (R_0^2 (1 + 2x + x^2) \varepsilon^2 - 12R_0^2 (1 + x) \dot{x} \varepsilon + 9R_0^2 (1 + x) \ddot{x} + 18R_0^2 \dot{x}^2) \left(\frac{R_0}{R_{c0}} - 1\right) + \frac{1}{2} (R_0^2 (1 + 2x + x^2) \varepsilon^2 - 6R_0^2 (\dot{x} + x\dot{x}) \varepsilon + 9R_0^2 \dot{x}^2) \left(\frac{R_0^4}{R_{c0}^4} - 1\right) \right). \quad (24) \end{aligned}$$

We neglected the non-linear terms of the above equation and rearrange it, setting $\alpha = R_0/R_{c0}$. Then we get the harmonic oscillation equation

$$\ddot{x}(t) + 2\beta \dot{x}(t) + \omega_0^2 x(t) = \psi - \frac{p_A \sin(\omega t)}{R_0^2 \rho (1 - \alpha)}, \quad (25)$$

where,

$$\psi = \frac{1}{(1 - \alpha)} \left(-\frac{\varepsilon^2}{18\alpha^2} + \frac{\varepsilon^2 \alpha}{9} - \frac{\varepsilon^2}{18} \alpha^4 \right),$$

$$\beta = \frac{1}{1 - \alpha} \left(\frac{2}{3} \varepsilon \alpha - \frac{\varepsilon \alpha^4}{6} - \frac{\varepsilon}{2} + \frac{2\mu}{\rho R_0^2} \right),$$

$$\begin{aligned} \omega_0^2 &= \frac{1}{R_0^2 (1 - \alpha)} \left(\frac{1}{\rho} \left(3K\alpha^3 + 3\gamma P_{g0} - \frac{2\sigma}{R_0} \right) + \varepsilon^2 \left(\frac{R_0^2}{9\alpha^2} + \frac{2R_0^2}{9} - \frac{2R_0^2 \alpha}{9} - \frac{R_0^2 \alpha^4}{9} \right) \right), \end{aligned}$$

and ω_0 is denoted as natural frequency. Note that, the equation is similarly reduced as in (Liu et al., 2018, Wang, 2017) when $\varepsilon \ll 1$. Equation (25) is known as harmonic oscillator (Nadir and Manmi, 2020) and can be solved analytically subject to appropriate initial radius and velocity. The exact solution of homogenous part of (25) can be classified into three cases.

1) If $\beta^2 > \omega_0^2$ then the general solution of (25) is

$$x_c = C_1 e^{-t(\beta + \sqrt{\beta^2 - \omega_0^2})} + C_2 e^{-t(\beta - \sqrt{\beta^2 - \omega_0^2})}$$

2) If $\beta^2 = \omega_0^2$ then the general solution in this case is

$$x_c = (C_1 + C_2 t) e^{-\beta t}$$

3) If $\beta^2 < \omega_0^2$ then the general solution of (29) is given by

$$x_c = C_1 e^{-\beta t} \cos(\omega_b t) + C_2 e^{-\beta t} \sin(\omega_b t),$$

where C_1 and C_2 are arbitrary constants and $\omega_b = \omega_0^2 - \beta^2$ can be found by using initial radius and velocity.

Particular solution of (25) can be found using D-operator method where P_A is considered as in (31) we arrive,

$$x_p = \frac{\psi}{\omega_0^2} - \frac{p_A}{\rho R_0^2(1-\alpha)((\omega_0^2 - \omega^2)^2 + 4\beta^2\omega^2)} ((\omega_0^2 - \omega^2)\sin(\omega t) - 2\beta\omega \cos(\omega t)),$$

where $P_A = p_A \sin(\omega t)$, ω is angular frequency and t is time. In the absence of wave pressure $p_A = 0$.

Thus, general solution of equation (25) is

$$x = x_c + x_p. \tag{26}$$

When $\epsilon = 0$ the general solutions in all above cases reduce same as in Rayleigh-Plesset equation (Bossio Castro, 2019).

4. NONDIMENSIONALIZATION

Nondimensionalization equations are a very well-known and useful technique in differential equations, particularly in fluid dynamics for simplifying the problem and reducing parameters. So, the physical units are removed and the variables are scaling. To dimensionless equation (21), we define $R = R_0 R_*$ be $\dot{R} = U \dot{R}_*$ and $\ddot{R} = \ddot{R}_* \frac{U^2}{R_0}$, $R_c = R_0 R_{c*}$ and $K = \Delta K_*$, where $U = \sqrt{\Delta/\rho}$ and $\Delta = P_\infty - p_v$, and the variables subscript with * denotes non-dimensional quantities (Wang and Manmi, 2014). By substituting $R, \dot{R}, \ddot{R}, R_c$ and K in equations (21) to see.

$$\begin{aligned} &\Delta K_* \alpha^3 (R_*^3 - 1) + P_\infty - p_v + P_A - P_{g0} \left(\frac{R_0}{R_0 R_*}\right)^{3\gamma} \\ &+ \frac{2\sigma}{R_0 R_*} + 4\mu \frac{\sqrt{\Delta} \dot{R}_*}{R_0 \sqrt{\rho} R_*} = -\frac{\rho}{9} \left(\frac{\epsilon^2 R_0^2 R_*^2}{2} \left(\left(\frac{R_{c*}}{R_*}\right)^2 - 1\right) + \left(\frac{9R_* \ddot{R}_* \Delta}{\rho} + \frac{18\Delta \dot{R}_*^2}{\rho} - \frac{12\epsilon R_0 R_* \sqrt{\Delta} \dot{R}_*}{\sqrt{\rho}}\right) \right. \\ &+ \epsilon^2 R_0^2 R_*^2 \left(1 - \frac{R_*}{R_{c*}}\right) + \left(\frac{3\epsilon R_0 R_* \dot{R}_* \sqrt{\Delta}}{\sqrt{\rho}} - \frac{9\dot{R}_*^2 \Delta}{2\rho} - \frac{\epsilon^2 R_0^2 R_*^2}{2} \left(1 - \frac{R_*^4}{R_{c*}^4}\right)\right), \end{aligned} \tag{27}$$

since Δ is different from zero we get

$$\begin{aligned} &K_* \alpha^3 (R_*^3 - 1) + 1 + \frac{P_A}{\Delta} - \frac{P_{g0}}{\Delta} R_*^{-3\gamma} + \frac{2\sigma}{\Delta R_0} R_*^{-1} \\ &+ 4 \frac{\mu}{\sqrt{\Delta} \rho R_0} \frac{\dot{R}_*}{R_*} = -\left(\frac{\epsilon^2 \rho R_0^2 R_*^2}{18 \Delta} \left(\left(\frac{R_{c*}}{R_*}\right)^2 - 1\right) \right. \\ &+ \left(R_* \ddot{R}_* + 2\dot{R}_*^2 - \frac{4\epsilon R_0 R_* \dot{R}_* \sqrt{\rho}}{3\sqrt{\Delta}} + \frac{\epsilon^2 R_0^2 R_*^2 \rho}{9\Delta}\right) \end{aligned} \tag{1}$$

$$\begin{aligned} &-\frac{R_*}{R_{c*}}) + \left(\frac{\epsilon R_0 R_* \dot{R}_* \sqrt{\rho}}{3\sqrt{\Delta}} - \frac{\dot{R}_*^2}{2} - \frac{\epsilon^2 R_0^2 R_*^2 \rho}{18\Delta}\right) \left(1 - \frac{R_*}{R_{c*}}\right) \\ &- \frac{R_*^4}{R_{c*}^4} \Big). \end{aligned} \tag{28}$$

Then, we get

$$\begin{aligned} &K_* \alpha^3 (R_*^3 - 1) + 1 + \frac{P_A}{\Delta} - \frac{P_{g0}}{\Delta} R_*^{-3\gamma} + \frac{2}{We} R_*^{-1} \\ &+ \frac{4}{Re} \frac{\dot{R}_*}{R_*} = -\left(\frac{\epsilon_*^2 R_*^2}{18} \left(\left(\frac{R_{c*}}{R_*}\right)^2 - 1\right) + (R_* \ddot{R}_* \right. \\ &+ 2\dot{R}_*^2 - \frac{4\epsilon_* R_* \dot{R}_*}{3} + \frac{\epsilon_*^2 R_*^2}{9}) \left(1 - \frac{R_*}{R_{c*}}\right) + \left(\frac{\epsilon_* R_* \dot{R}_*}{3} \right. \\ &\left. - \frac{\dot{R}_*^2}{2} - \frac{\epsilon_*^2 R_*^2}{18}\right) \left(1 - \frac{R_*^4}{R_{c*}^4}\right). \end{aligned} \tag{29}$$

where $\epsilon_* = R_0 \sqrt{\rho/\Delta} \epsilon$, $Re = \frac{R_0 \sqrt{\rho} \Delta}{\mu}$ and $We = \frac{R_0 \Delta}{\sigma}$.

5. NUMERICAL RESULTS AND DISCUSSION

In this section, gas and acoustic bubble oscillations characterized by the parameters $\mu = 0.001$ Pa s, $\rho = 1000$ kg m⁻³, $\sigma = 0.05$ N m⁻¹, $P_v = 2.3$ kPa, $P_\infty = 100$ kPa, $P_{g0} = 0.001$, $R_0 = 5 \mu\text{m}$, $\alpha = \frac{1}{4}$, $K = 10^8$, $p_{g0} = 117.7$ kPa and $\epsilon_* = 0, 0.04$ and 0.08 have been considered. Equation (21) is the nonlinear second order differential equation that cannot be solved analytically (Nadir and Manmi, 2020). However, it can be solved by using an efficient numerical approach such as fourth order Runge-Kutta scheme (RK4) (Saeed and Sadeeq, 2017) for a linear system of the ordinary differential equation (LSODE). To change equation (29) to LSODE we assume $y_1 = R_*$, $y_2 = \dot{y}_1$, which leads us to

$$\begin{aligned} &\dot{y}_1 = y_2, \\ &\dot{y}_2 = -\frac{1}{y_1(1-\alpha)} \left(K_* \alpha^3 (y_1^3 - 1) + 1 + \frac{P_A}{\Delta} - \frac{P_{g0}}{\Delta} y_1^{-3\gamma} + \frac{2}{We} y_1^{-1} + \frac{4}{Re} \frac{y_2}{y_1} + \frac{\epsilon_*^2 y_1^2}{18} \left(\left(\frac{1}{\alpha}\right)^2 - 1\right) \right. \\ &+ \left(2y_2^2 - \frac{4\epsilon_* y_1 y_2}{3} + \frac{\epsilon_*^2 y_1^2}{9}\right) (1-\alpha) + \left(\frac{\epsilon_* y_1 y_2}{3} - \frac{y_2^2}{2} - \frac{\epsilon_*^2 y_1^2}{18}\right) (1-\alpha^4). \end{aligned} \tag{30}$$

In this work, MATLAB function ode45 which is based on fourth order Runge Kutta method with

controlling the maximum step (0.01) and relative error (0.05) was used for solving the above system (Yi and Lu, 2017, 2018, Mathworks, 2018, Bossio Castro, 2019).

5.1 Comparison Between Solution of Linearization and Nonlinear

Figures 2a and 2b show the comparison of the numerical and exact solutions of bubble radius oscillations subject to the acoustic wave with different ϵ_* . It is observed that, the bubble radius over time was not affected significantly when $\epsilon_* = 0.04$, while when $\epsilon_* = 0.08$, the effects of ϵ_* on the frequency and amplitude of bubble oscillations increases over time. Therefore, when ϵ_* is increasing, the difference between linearization and the numerical solution is increasing in all cycles with the same parameters as the pervious.

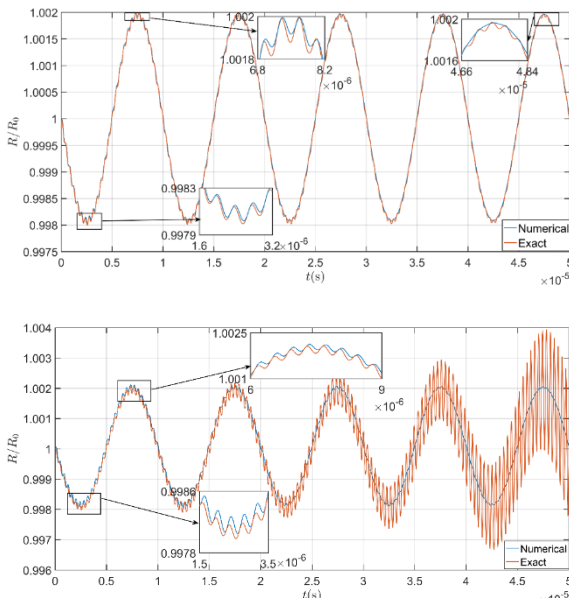


Fig 2. Comparison the numerical (30) and exact solutions (29) of bubble radius in elastic confinement when (a) $\epsilon_* = 0.04$ and (b) $\epsilon_* = 0.08$, the remaining parameters are $\mu = 0.001$ Pa s, $\rho = 1000$ kg m⁻³, $\sigma = 0.05$ N m⁻¹, $p_v = 2.3$ kPa, $P_\infty = 100$ kPa, $R_0 = 5$ μ m, $\alpha = 1/4$, $K = 10^8$ and $p_{g0} = 117.7$ kPa..

5.2 Gas Bubble Oscillations

In this section confined gas bubble oscillation was performed for different α, ϵ_*, K to investigate the effect of these parameters. The considered cases are characterised by the following parameters $\mu = 0.001$ Pa s, $\rho = 1000$ kg m⁻³, $\sigma = 0.05$ N m⁻¹, $P_A = 0$, $p_v = 2.3$ kPa, $P_\infty = 100$ kPa, $P_{g0} = 0.001$ and $R_0 = 5$ μ m. Figure 3 shows bubble radius oscillations when $\epsilon_* = 0$ (solid blue), 0.04 (solid red) and 0.08 (solid yellow) with $R_0/R_{c0} = 1/4$.

Figures 3 show the comparison of the bubble radius oscillations subject to the acoustic wave with different ϵ_* . It is observed that the bubble radius over time is increasing with ϵ_* when $\epsilon_* = 0$ to 0.04 the bubble radius increases 0.062% from R_{max} and R_{min} respectively. while when ϵ_* in increasing from 0.04 to 0.08, the effects of ϵ_* on the frequency and amplitude of bubble radius oscillations increase over time by about 0.4% of R_{max} and R_{min} respectively. Nevertheless, when ϵ_* is increasing, the difference between the radius of oscillations is increasing in all cycles of time.

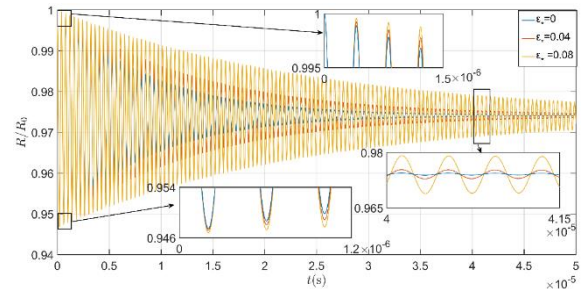


Fig 3. The comparison of the bubble radius when the parameters used are $\epsilon_* = 0, 0.04$ and 0.08 for $\alpha = 1/4$, $K = 10^8$. The other parameters are $R_0 = 5$ μ m, $P_A = 0$, $p_v = 2.3$ kPa, $P_\infty = 10^5$ Pa, $P_{g0} = 0.001$, $\mu = 0.001$ Pa s, $\rho = 1000$ kg m⁻³ and $\sigma = 0.05$ N m⁻¹.

5.3 Acoustic Bubble Oscillations

The propagation of pressure oscillations with sound velocity through a medium such as solid, liquid, or gas is known as an acoustic wave (sound) (Yasui, 2018). Stable bubbles can be activated by acoustic waves. In the presence of a standing acoustic wave, the acoustic pressure in (21) can be expressed as

$$P_A = p_A \sin(\omega t), \tag{31}$$

where p_A is the pressure amplitude and ω is the angular frequency. To consider the effect of ϵ_* in equation (21) in acoustic bubble oscillation $\epsilon_* = 0, 0.04$ and 0.08 with the parameters are $\alpha = 1/4$, $K = 10^8$, $R_0 = 5$ μ m, $p_v = 2300$ pa, $P_\infty = 10^5$ Pa, $P_{g0} = 117.7$ kPa, $\mu = 0.001$ Pa, $\rho = 1000$ kg m⁻³, $\sigma = 0.05$ N m⁻¹. Figure 3 illustrates bubble radius oscillation along 50 μ s. The maximum bubble radius decreases and the minimum bubble radius increases with increasing ϵ_* . However, the average bubble radius over the considered period was not changed significantly with ϵ_* .

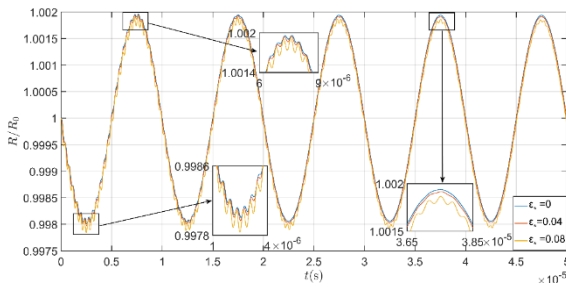


Fig. 4. Comparison of the bubble radius by ϵ_* versus time for the acoustic wave from the parameters are $\epsilon_* = 0, 0.04$ and 0.08 and the remaining parameters are $K = 10^8$, $\alpha = 1/4$, $R_0 = 5 \mu\text{m}$, $p_v = 2300 \text{ pa}$, $p_\infty = 10^5 \text{ Pa}$, $p_{g0} = 117.7 \text{ kPa}$, $p_A = 10 \text{ kPa}$, $\omega_a = 200 \text{ kPa}$, $\mu = 0.001 \text{ Pa s}$, $\rho = 1000 \text{ kg m}^{-3}$ and $\sigma = 0.05 \text{ N m}^{-1}$.

The dual-frequency bubble for equation (28) can be written as a combination of two waves

$$P_A = (P_{a1} \sin(\omega_1 t) + P_{a2} \sin(\omega_2 t + \phi)),$$

where P_{a1} and P_{a2} are the pressure amplitudes, ω_1 and ω_2 are the angular frequency and ϕ is the phase shift of the wave (Klapcsik, 2021, Hu et al., 2019, Saitoh et al., 1995).

When $P_{a1} = P_{a2} = p_A/2 = 5 * 10^3$, $\omega_1 = \omega_2 = 200 \text{ kHz}$, and $\phi = 0$, we obtain the same as in Figure 3. Here, the parametric study has the same parameters as Figure 3 except $P_{a1} = 80 \text{ kPa}$, $P_{a2} = 40 \text{ kPa}$, $\omega_1 = 200 \text{ kHz}$ and $\omega_2 = 210 \text{ kHz}$. In this figure, the maximum radius in all cycles was increased by about 0.005% and 0.02% for $\epsilon_* = 0.04$ and $\epsilon_* = 0.08$ respectively. However, the minimum bubble radius was not changed significantly in all cycles.

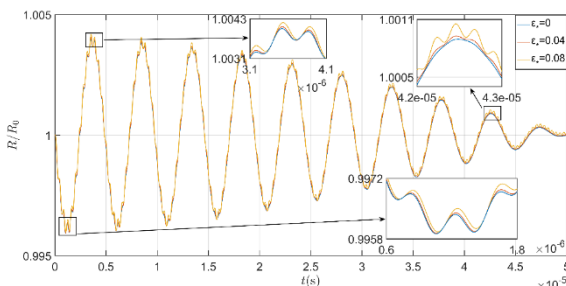


Fig 5: The bubble radius shows the defect of the different ϵ_* where $\epsilon_* = 0$ (blue solid), 0.04 (red solid) and 0.08 (yellow solid) versus time on the acoustic wave with the parameters are $P_\infty = 100 \text{ kPa}$, $p_v = 2.3 \text{ kPa}$, $R_0 = 5 \mu\text{m}$, $\mu = 0.001 \text{ Pa s}$, $\sigma = 0.05 \text{ N m}^{-1}$, $\alpha = 1/4$, $K = 10^8$, $P_{g0} = 117.7 \text{ kPa}$, $\rho = 1000 \text{ kg m}^{-3}$, $P_{a1} = 80 \text{ kPa}$, $P_{a2} = 40 \text{ kPa}$, $\omega_1 = 200 \text{ kHz}$ and $\omega_2 = 210 \text{ kHz}$.

6. SUMMARY AND CONCLUSIONS

By modifying the Ryleigh-Plesset equation for spherical bubble oscillations in Newtonian and viscous fluid with considering compressibility parameter ϵ in a spherical liquid-filled elastic solid

was derived and analysed. The equation is linearized for a small amplitude of oscillations. Then, the exact solution of the linearization is compared with the numerical solution of the original equation. It is observed that when $\epsilon_* = 0.08$, the difference between the exact and numerical solution is increasing over time, while when ϵ_* is smaller than 0.08 the difference does not change any cycles. However, the amplitude of the bubble radius oscillation is increasing with ϵ_* . Then the effect of ϵ_* is increasing over time.

References

ACHESON, D. J. 1991. Elementary fluid dynamics. Acoustical Society of America.

ARITAN, S. 2006. Bulk Modulus.

BATCHELOR, C. K. & BATCHELOR, G. 2000. *An introduction to fluid dynamics*, Cambridge University Press.

BOSSCHERS, J. 2018. Propeller tip-vortex cavitation and its broadband noise.

BOSSIO CASTRO, A. 2019. *LAGRANGIAN TRACKING OF THE CAVITATION BUBBLE (Master thesis)*.

COCHARD, H. 2006. Cavitation in trees. *Comptes Rendus Physique*, 7, 1018-1026.

CRUM, L. A., MASON, T. J., REISSE, J. L. & SUSLICK, K. S. 1998. *Sonochemistry and sonoluminescence*, Springer Science & Business Media.

DOINIKOV, A. A., DOLLET, B. & MARMOTTANT, P. 2018a. Cavitation in a liquid-filled cavity surrounded by an elastic medium: Intercoupling of cavitation events in neighboring cavities. *Physical Review E*, 98, 013108.

DOINIKOV, A. A., DOLLET, B. & MARMOTTANT, P. 2018b. Model for the growth and the oscillation of a cavitation bubble in a spherical liquid-filled cavity enclosed in an elastic medium. *Physical Review E*, 97, 013108.

DRYSDALE, C., DOINIKOV, A. A. & MARMOTTANT, P. 2017. Radiation dynamics of a cavitation bubble in a liquid-filled cavity surrounded by an elastic solid. *Physical Review E*, 95, 053104.

DURYEA, A. P., ROBERTS, W. W., CAIN, C. A. & HALL, T. L. Optimization of histotripsy for kidney stone erosion. 2010 IEEE International Ultrasonics Symposium, 2010. IEEE, 342-345.

DURYEA, A. P., ROBERTS, W. W., CAIN, C. A. & HALL, T. L. 2015. Removal of residual cavitation nuclei to enhance histotripsy erosion of model urinary stones. *IEEE transactions on ultrasonics, ferroelectrics, and frequency control*, 62, 896-904.

FRANC, J.-P. & MICHEL, J.-M. 2006. *Fundamentals of cavitation*, Springer science & Business media.

HU, A., LI, Y. & ZHENG, J. 2019. Dual-frequency ultrasonic effect on the structure and properties of starch with different size. *LWT*, 106, 254-262.

JENSEN, K. H., BERG-SØRENSEN, K., BRUUS, H., HOLBROOK, N. M., LIESCHE, J., SCHULZ, A.,

- ZWIENIECKI, M. A. & BOHR, T. 2016. Sap flow and sugar transport in plants. *Reviews of modern physics*, 88, 035007.
- KELLER, J. B. & KOLODNER, I. I. 1956. Damping of underwater explosion bubble oscillations. *Journal of applied physics*, 27, 1152-1161.
- KLAPCSIK, K. 2021. GPU accelerated numerical investigation of the spherical stability of an acoustic cavitation bubble excited by dual-frequency. *Ultrason Sonochem*, 77, 105684.
- KORKUT, E. & ATLAR, M. 2012. An experimental investigation of the effect of foul release coating application on performance, noise and cavitation characteristics of marine propellers. *Ocean Engineering*, 41, 1-12.
- LARTER, M., BRODRIBB, T. J., PFAUTSCH, S., BURLETT, R., COCHARD, H. & DELZON, S. 2015. Extreme aridity pushes trees to their physical limits. *Plant Physiology*, 168, 804-807.
- LAUTERBORN, W. & KURZ, T. 2010. Physics of bubble oscillations. *Reports on progress in physics*, 73, 106501.
- LIU, Y., WANG, Q. & ZHANG, A.-M. 2018. Surface stability of a bubble in a liquid fully confined by an elastic solid. *Physics of Fluids*, 30, 127106.
- MARION, M. & TEMAM, R. 1998. Navier-Stokes equations: Theory and approximation. *Handbook of numerical analysis*, 6, 503-689.
- MATHWORKS 2018. *Matlab R2018b User's Guide*.
- NADIR, N. N. & MANMI, K. M. 2020. Comparative Investigation of the Spherical Acoustic Microbubble Models in an Unbounded Liquid. *Zanco Journal of Pure and Applied Sciences*, 32, 82-88.
- NIGMATULIN, R., AKHATOV, I. S., VAKHITOVA, N. & LAHEY, R. 1999. Hydrodynamics, acoustics and transport in sonoluminescence phenomena. *Sonochemistry and Sonoluminescence*. Springer.
- PLESSET, M. S. & PROSPERETTI, A. 1977. Bubble dynamics and cavitation. *Annual review of fluid mechanics*, 9, 145-185.
- RAYLEIGH, L. 1917. VIII. On the pressure developed in a liquid during the collapse of a spherical cavity. *The London, Edinburgh, and Dublin Philosophical Magazine and Journal of Science*, 34, 94-98.
- SAEED, R. & SADEEQ, M. I. 2017. Radial Basis Function-Pseudospectral Method for Solving Non-Linear Whitham-Broer-Kaup Model. *Sohag Journal of Mathematics*, 4, 13-18.
- SAITOH, S., IZUMI, M. & MINE, Y. 1995. A dual frequency ultrasonic probe for medical applications. *IEEE transactions on ultrasonics, ferroelectrics, and frequency control*, 42, 294-300.
- STROOCK, A. D., PAGAY, V. V., ZWIENIECKI, M. A. & HOLBROOK, N. M. 2014. The physicochemical hydrodynamics of vascular plants. *Annu. Rev. Fluid Mech*, 46, 615-642.
- TYREE, M. T. & SPERRY, J. S. 1989. Vulnerability of xylem to cavitation and embolism. *Annual review of plant biology*, 40, 19-36.
- WANG, Q. 2017. Oscillation of a bubble in a liquid confined in an elastic solid. *Physics of Fluids*, 29, 072101.
- WANG, Q. & MANMI, K. 2014. Three dimensional microbubble dynamics near a wall subject to high intensity ultrasound. *Physics of Fluids*, 26, 032104.
- YASUI, K. 2018. *Acoustic cavitation and bubble dynamics*, Springer.
- YI, J. & LU, Y. 2017. Effects of vapour pressure on the motion of cavitation bubble. *Physics and Chemistry of Liquids*, 55, 1-10.
- YUSOF, N. S. M., ANANDAN, S., SIVASHANMUGAM, P., FLORES, E. M. & ASHOKKUMAR, M. 2022. A correlation between cavitation bubble temperature, sonoluminescence and interfacial chemistry—A minireview. *Ultrasonics Sonochemistry*, 105988.
- ZHOU, M., YUSOF, N. S. M. & ASHOKKUMAR, M. 2013. Correlation between sonochemistry and sonoluminescence at various frequencies. *RSC advances*, 3, 9319-9324.